Carbon Dioxide Fixation by Lithium Amides: DFT Studies on the Reaction Mechanism of the Formation of Lithium Carbamates

Sten O. Nilsson Lill,*[a] Uwe Köhn,[b] and Ernst Anders*[b]

Keywords: Carbon dioxide fixation / Chiral lithium amides / Density functional calculations / Heterodimers / Reaction mechanisms

A realistic picture of the complete insertion reaction for a representative example of the formation of carbamates from lithium amides is given by combining experimental information with detailed DFT investigations. The chiral lithium (*S*)-2-(pyrrolidin-1-ylmethyl)pyrrolidide (**2**) reacts with CO_2 to form its corresponding carbamate. In this reaction the second pyrrolidine ring functions as an intramolecular ligand, and therefore, "symmetrical" as well as "unsymmetrical" dimers of **2** have to be taken into account. On the energetically preferred reaction pathway this amide exists predominantly as a (solvated) dimer **4**. Attack by CO_2 occurs in an "end-on" manner to give several heterodimers **5** which are composed of a lithium amide and a lithium carbamate. This exergonic step is rate determining, and the activation barrier was estimated to be about 10 kcal mol^{-1}. A second lithium-mediated CO_2 insertion into a nitrogen–lithium bond yields the encounter complex **5d–(CO_2)**, which then goes on to form several almost isoenergetic homodimeric carbamates **6**. This strongly exergonic insertion reaction has a barrier of 9.7 kcal mol^{-1}. We also report on novel lithium-mediated CO_2 insertion reactions into oxygen–lithium bonds in lithium carbamates.

(© Wiley-VCH Verlag GmbH & Co. KGaA, 69451 Weinheim, Germany, 2004)

Introduction

Is the formation of carbamates from lithium amides and CO_2 a simple story? By no means! One only needs to consider the important aspects of aggregation/disaggregation as well as microsolvation of the species involved (starting materials, intermediates, transition structures and products). Organic carbamates are important intermediates in the synthesis of a number of drugs,[1–5] agricultural chemicals (e.g. Carbaryl and Propoxur) and fuel additives, and are also involved in fatty acid synthesis by means of biotin-dependent carbon dioxide fixation.[6] However, the synthesis of carbamates by traditional procedures requires the use of phosgene or isocyanates, which are toxic compounds. Recently, carbamates have been generated through *N*- or *O*-alkylations with caesium bases, or through electrochemical synthesis from amines and carbon dioxide.[7–10] In an alternative procedure of carbon dioxide fixation recently presented by us, easily accessible chiral lithium amides[11] and CO_2 were used for the first time for the synthesis of *chiral* carbamates (Scheme 1).[12] The chiral lithium carbamates are aimed to be used in novel CO_2 transfer reactions to prochiral carbon atoms,[13–15] for example to prochiral ketone enolates for enantioselective synthesis of β-keto acids which are important precursors in medicinal chemistry.[16,17]

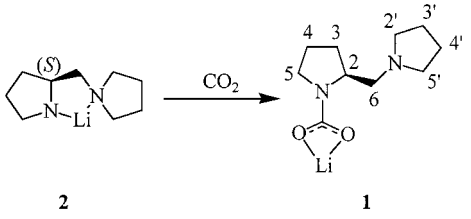

2 **1**

Scheme 1. Formation of lithium carbamate **1** from lithium amide **2** and carbon dioxide

In our previous study several chiral lithium carbamates were characterised by cryoscopy, NMR spectroscopy and computational chemistry.[12] In this study, we report on DFT investigations on possible *reaction mechanisms* for the formation of lithium carbamates from CO_2 and lithium amides. As a model we have chosen the formation of lithium carbamate **1** from lithium (*S*)-2-(pyrrolidin-1-ylmethyl)pyrrolidide (**2**, see Scheme 1), an example of a useful reagent

[a] Present Address: Department of Chemistry, Göteborg University,
Kemigården 3, 412 96 Göteborg, Sweden
Fax: (internat.) + 46-31-7723840
E-mail: stenil@chem.gu.se
[b] Institut für Organische Chemie und Makromolekulare Chemie der Friedrich-Schiller-Universität,
Lessingstrasse 8, 07743 Jena, Germany
Fax: (internat.) + 49-3641-948212
E-mail: Ernst.Anders@uni-jena.de

Supporting information for this article is available on the WWW under http://www.eurjoc.org or from the author.

 © 2004 Wiley-VCH Verlag GmbH & Co. KGaA, Weinheim **DOI: 10.1002/ejoc.200400163**

derived from proline and used in asymmetric synthesis.[18−24]

Computational Details

All compounds were optimised by using Gaussian 98.[25] All stationary points were characterised as minima or TSs by the sign of the eigenvalues of the force-constant matrix obtained from a frequency calculation. Optimised TSs with one imaginary frequency were confirmed to describe the correct displacement by a normal-mode analysis using Molden.[26] In general, compounds were optimised with the hybrid density functional B3LYP[27,28] and two different basis sets: Ahlrichs' SVP[29] and Pople's 6−31+G(d).[30−33] Free energy correction terms were, if not otherwise stated, taken from frequency calculations at 298.15 K and 1 atm pressure at the B3LYP/SVP (BI) level of theory.[34] To obtain the estimated free energy at the B3LYP/6-31+G(d) (BII) level of theory the SVP-calculated correction term was added to the 6−31+G(d)-calculated potential energy. Some compounds were also optimised using either MP2/6-31+G(d)[35] (MII) or MP2/6-311+G(d,p) (MIII) with the frozen-core approximation, or alternatively using mPW1K/6-31+G(d)[36] (mPWII) or mPW1K/6-311+G(d,p) (mPWIII). Generally, energies given in the text are at the BII/BI level.

Results and Discussion

Lithiated organic compounds are known to form dynamic aggregates whose size is dependent on the solvent used, the steric requirements of the substituents on the lithium amide and the temperature.[37−41] Such aggregates have been well investigated by colligative measurements, NMR spectroscopy, and X-ray and computational studies.[42−53] In order to elucidate the composition of the lithium amide reactant **2** involved in the formation of lithium carbamate **1**, results on its aggregation and solvation are presented in the first paragraph.

Lithium Amide Aggregation

NMR spectroscopic studies by Ahlberg and co-workers have shown that a dimer **3** of **2** (Figure 1) is preferred in ethereal solvents in the presence of, for example, *N*,*N*,*N*′,*N*′-tetramethylethylenediamine (TMEDA).[44] In **3**, one lithium atom [Li(1)] is intramolecularly tetracoordinated, while the other [Li(2)] is dicoordinated, thus making the lithium atoms non-equivalent. In another dimer of **2**, **4** (Figure 1), the two lithium atoms are equivalent. In THF solution it has been found that a number of different aggregates of **2** are involved in dynamic processes.[44]

In this study, we have optimised the geometries of dimers **3** and **4** at the BII level of theory. It is found that the previously reported PM3-optimised geometry of dimer **3** shows significant deviations from the B3LYP-optimised geometry.[44] For example, the N(2)−Li(2) bond length in **3** is longer calculated with PM3 than with BII (see Table 1 and Figure 1). In addition, the Li−Li distance is distinctly different at these levels (DFT: 2.34 Å and PM3: 2.64 Å). The N−Li bond lengths in **3** and **4** optimised with BII and with BI are in good agreement (Table 1), which justifies the use of the latter method for geometry optimisations of larger aggregates and of solvated compounds. As a further validation of the methods, optimisations of the dimer of lithium *N*,*N*-dimethylamide at the MP2 and mPW1K levels of theory were performed (Table 1). These results confirm that the PM3 method gives very long N−Li and Li−Li distances, while the DFT and MP2 results are in very good agreement. This shows that the BI-optimised geometries are adequate to use.

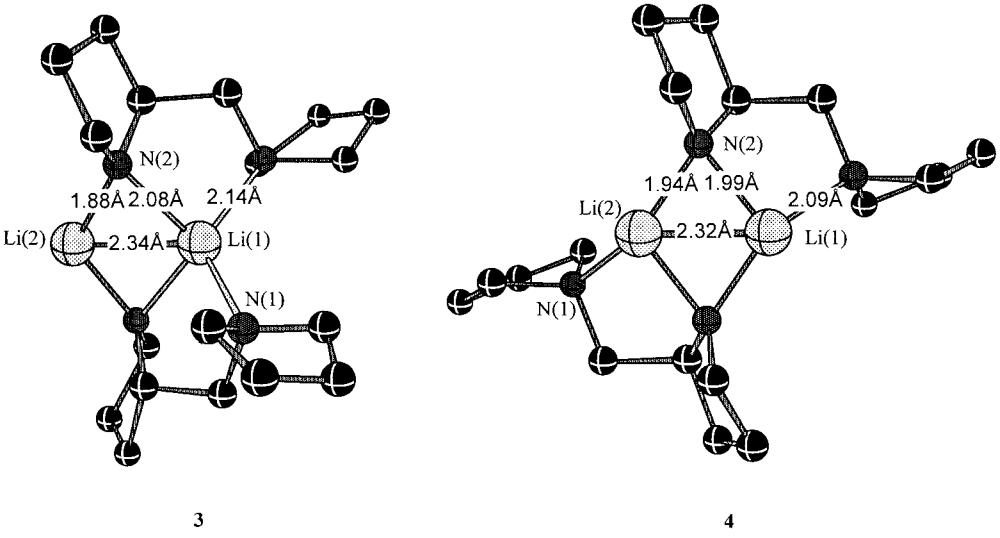

3 **4**

Figure 1. Optimised lithium amide dimers **3** and **4**; For basis sets and relative energies: See text and cf. Table 3 and Scheme 4

 © 2004 Wiley-VCH Verlag GmbH & Co. KGaA, Weinheim

Table 1. Selected bond lengths (Å) of lithium amide dimers **3**, **4** and $LiN(CH_3)_2$ using different methods; for method abbreviations see Computational Details)

Structure	PM3	BI	BII	MII	MIII	mPWII	mPWIII
3							
N(2)−Li(2)	2.01	1.91	1.88				
N(2)−Li(1)	2.09	2.09	2.08				
N(1)−Li(1)	2.18	2.16	2.14				
Li−Li	2.64	2.37	2.34				
4							
N(2)−Li(2)	2.02	1.97	1.94				
N(2)−Li(1)	2.05	2.01	1.99				
N(1)−Li(2)	2.13	2.11	2.09				
Li−Li	2.58	2.36	2.32				
$LiN(CH_3)_2$							
N−Li	2.01	1.96	1.94	1.96	1.96	1.93	1.93
Li−Li	2.38	2.30	2.27	2.30	2.31	2.27	2.26

Table 3. Calculated relative Gibbs free energies [kcal mol^{-1}] of dimers **3** and **4** (free and CO_2 and/or THF solvated) and the transition structures **TS1**−**TS4**

Structure	BII//BII	BII//BI	BI//BI
4	0	0	0
3	+3.9	+3.6	+3.3
4−(THF)	+0.1	+0.6	−4.1
4a−$(THF)_2$	−	+7.2	−1.8
4b−$(THF)_2$	−	−	+7.9
3−(THF)	+2.5	+2.0	−1.9
3−$(THF)_2$	−	+12.1	+3.6
3−(CO_2)		+8.6	+5.2
3a−(CO_2)−(THF)		+12.5	+5.4
3b−(CO_2)−(THF)		+12.0	+5.6
4−(CO_2)		+9.7	+6.5
4−(CO_2)−(THF)		+17.0	+9.6
TS1		+9.9	+6.5
TS2		+16.1	+8.4
TS3		+11.8	+8.5
TS4		+19.6	+12.0

However, although BI calculations might give accurate geometries, it has been stated that to obtain acceptable *energies* for lithiated compounds, a basis set including diffuse functions is needed.[54,55] This is especially true when using density functional theory.[56] In order to explore this, we have, at various levels of theory, calculated the dimerisation energy for the model compound $LiN(CH_3)_2$ and the solvation energy resulting from specific coordination with a dimethyl ether molecule (Table 2).

There is an excellent agreement between the BII/BI, MIII//MIII and mPWIII//mPWIII calculated dimerisation energies, while the solvation energies calculated using the BI/BI approach are more consistent with the MII//MII and mPWIII//mPWIII values than those calculated at the BII/BI level. Overall, the BII/BI energies seem to be the most efficient alternative to use.

For our main system, we have compared relative free energies calculated with the BI//BI, BII//BI and BII//BII approaches (see Table 3). Dimer **4** is calculated to be 3.9 kcal mol^{-1} more stable than dimer **3** at the BII//BII level. Similar free energy differences are found at both the BII//BI and BI//BI level of theory (Table 3).

To investigate the role of solvation of **3** and **4**, specific coordination of THF molecules was performed (Figure 2). In **3**, only the dicoordinated Li(2) was considered for solvation, while in **4** both lithium cations were considered, because they are equivalent.

The free energies of solvation (ΔG_{sol}) calculated at the BII//BII level of theory is found to be −1.4 kcal mol^{-1} for **3** and +0.1 kcal mol^{-1} for **4**. It is observed that ΔG_{sol} is larger for **3** than for **4**, meaning that with a sufficiently powerful solvent the solvated dimer **3** will eventually be the dominating species, in line with the observations of the TMEDA solvated dimer **3**.[44] Both the BII//BI and BI//BI approaches indicate that disolvation of **3** and **4** are predicted to be endergonic processes. Such structures are assembled in the Supporting Information. Due to the small solvation energies of **4** and the uncertainties in the accuracy of the DFT functional used, it is predicted that the unsolvated isomer **4** together with **4−(THF)** are in equilibrium with both **4−$(THF)_2$** and the isomer **3−(THF)** (Figure 2).

Although the degree of solvation of the lithium amide reactant **2** could not be determined computationally due to this equilibrium, we show in the next section that addition of carbon dioxide will result in relatively large kinetic differences between reaction paths involving solvent molecules and those in which solvent molecules are not involved.

Addition of Carbon Dioxide

Addition of one molecule of CO_2 to dimer **4** initially results in the formation of the encounter complex **4−(CO_2)**, in which one lithium cation coordinates the CO_2 molecule (Figure 3). The free energy value resulting from this addition is calculated to be about +10 kcal mol^{-1}; at the BII//BI level of theory this is thus an endergonic process. Similarly, addition of CO_2 to the dimer **3** gives the encounter complex **3−(CO_2)** (Figure 3). The two isomers **3−(CO_2)** and **4−(CO_2)** are close in terms of free energy; the difference is only about 1 kcal mol^{-1} in favour of **3−(CO_2)**.

Addition of THF to the most stable CO_2 solvated dimer **3−(CO_2)** leads to **3−(CO_2)−(THF)** (Figure 4). Two almost

Table 2. $LiN(CH_3)_2$: Calculated dimerisation and solvation energies [kcal mol^{-1}]

Energy	BI//BI	BII/BI	BII//BII	MII//MII	MIII/MIII	mPWII//mPWII	mPWIII//mPWIII
Dimerisation energy	−66.20	−57.60	−57.34	−59.90	−57.76	−60.26	−57.64
Solvation energy	−17.49	−14.72	−14.60	−21.74	−	−15.32	−17.18

 © 2004 Wiley-VCH Verlag GmbH & Co. KGaA, Weinheim

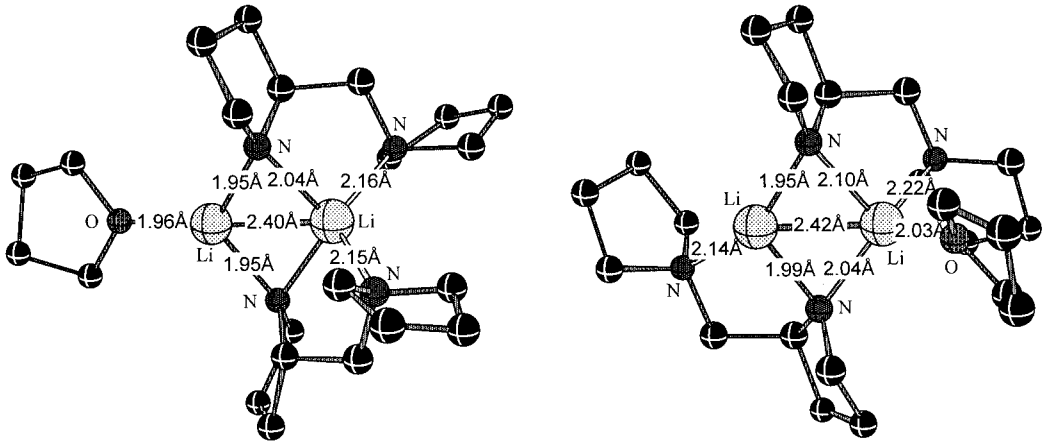

Figure 2. Optimised monosolvated lithium amide dimers

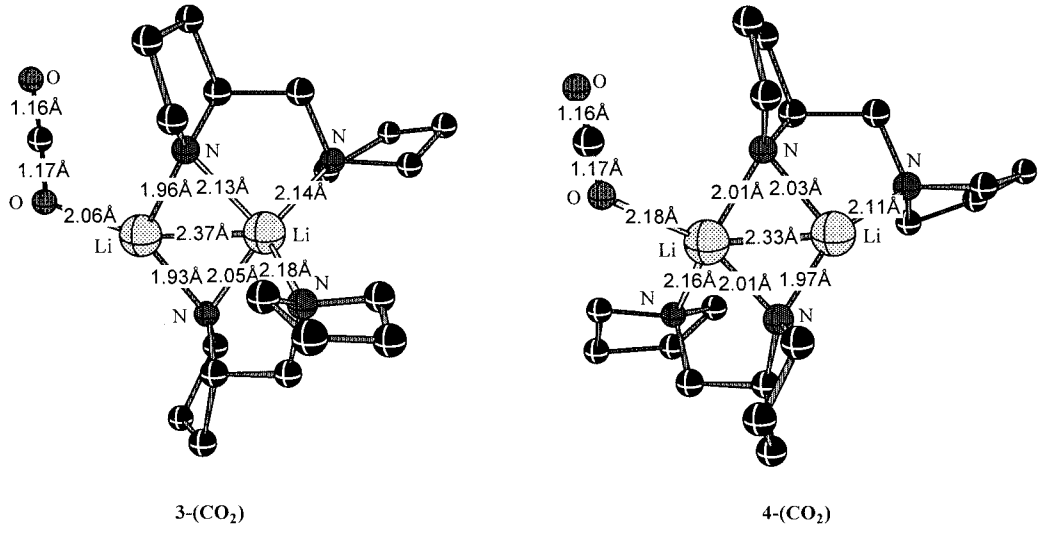

Figure 3. Optimised encounter complexes of dimeric lithium amides with CO_2

isoenergetic isomers, **3a−(CO$_2$)−(THF)** and **3b−(CO$_2$)−(THF)**, mainly differing in the orientation of the CO_2 moiety, were located on the potential energy surface (PES). In both isomers the CO_2 molecule is weakly bonded to Li(2), and thus the distortions of CO_2 in the encounter complexes are found to be small relative to uncoordinated CO_2. The solvation energies are found to result in an equilibrium between the encounter complex **3−(CO$_2$)** and its solvated counterparts, while **4−(CO$_2$)** is probably not solvated in THF.

Transition Structures for CO_2 Insertion into the N−Li Bond

By gradually reducing the distance between the electrophilic carbon atom in carbon dioxide and the nucleophilic amidic nitrogen atom in the most stable encounter complex **3−(CO$_2$)**, a TS for carbamate formation, **TS1**, was detected (Figure 5). The CO bond lengths in **TS1** and the OCO angle (170°) are indicative of an attack at the central carbon atom. Only small changes in the N−Li bonds are detected on going from **3−(CO$_2$)** to **TS1**, indicating an early TS on the reaction coordinate.

Since **TS1** is found to be only 1.3 kcal mol^{-1} less stable than the complex **3−(CO$_2$)** (Table 3), *once the encounter complex has been formed the product formation is almost barrierless.* Attempts to locate a TS from the encounter complex **4−(CO$_2$)** resulted in **TS3**. This TS has a free energy barrier of 2.1 kcal mol^{-1} from **4−(CO$_2$)**. Comparison of the free energies of the TSs with those of the separate reactants (dimer **4**, CO_2 and THF) shows that the lowest activation barriers are found for the *unsolvated* TSs **TS1** and **TS3** in which THF had previously dissociated. The sol-

 © 2004 Wiley-VCH Verlag GmbH & Co. KGaA, Weinheim

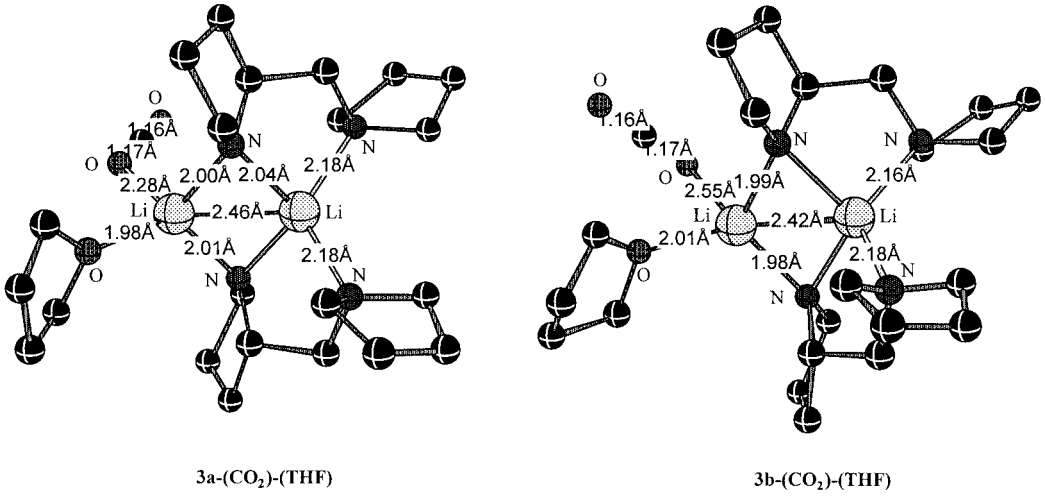

Figure 4. Optimised isomers of THF solvated encounter complexes, cf. Figure 3

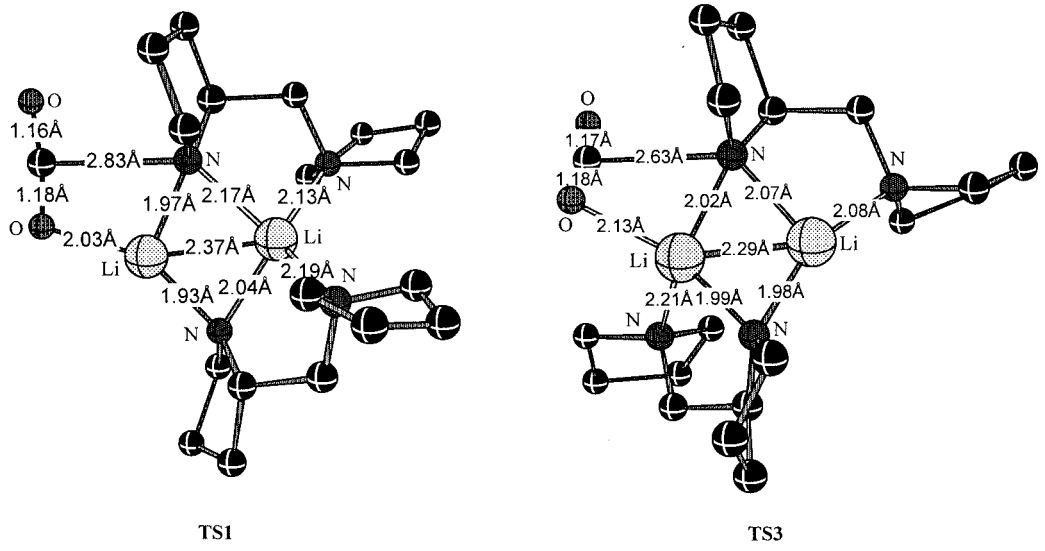

Figure 5. Optimised transition structures: **TS1** for insertion of CO_2 into an N−Li bond of **3−(CO$_2$)**, or **TS3** for the analogues insertion into **4-(CO$_2$)**, cf. Figure 3

vated TSs **TS2** and **TS4** are given in the Supporting Information. According to the energies of **TS1** (+9.9 kcal mol^{-1}) and **TS3** (+11.8 kcal mol^{-1}), it is likely that both will contribute to product formation but **TS1** will predominate over **TS3**. The activation barriers are low, in accordance with the experiments that show that after addition of CO_2 to a lithium amide solution, carbamate formation is completed rapidly (<1 h) at room temperature.[12] Thus, although reactant **4** is thermodynamically in equilibrium with the solvated species **4−(THF)**, the *unsolvated* encounter complexes **3−(CO$_2$)** and **4−(CO$_2$)** are kinetically preferred according to the DFT calculations presented here.

Heterodimer Formation

The product formations from the located TSs are found to be stepwise and exergonic processes. Initially, a heterodimer **5** composed of one lithium amide monomer and one lithium carbamate monomer is formed (Scheme 2 and Figure 6). The most stable isomers of **5** are given in Figure 6; others can be found in the Supporting Information.

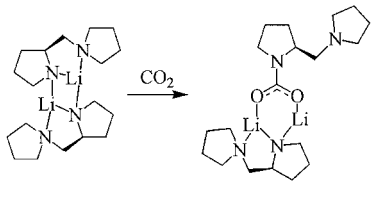

Scheme 2. Formation of heterodimer **5** from lithium amide dimer **4** and carbon dioxide

 © 2004 Wiley-VCH Verlag GmbH & Co. KGaA, Weinheim

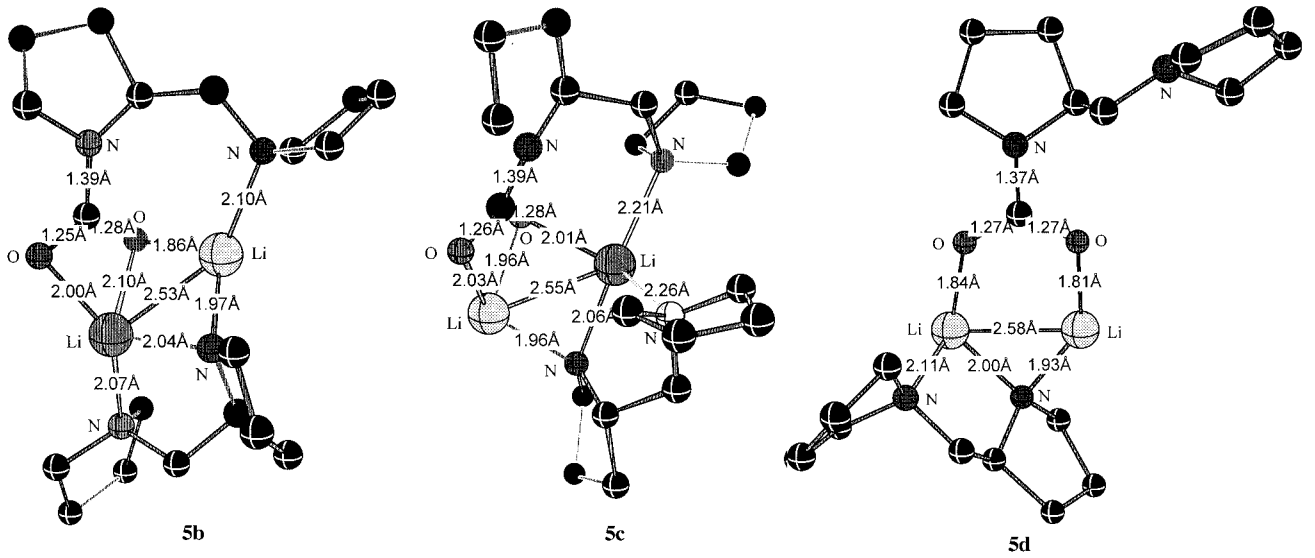

Figure 6. Optimised isomers of the heterodimer **5**

The most stable TS (**TS1**) results in isomer **5b**, while **TS3** results in isomer **5c** (Figure 6). Several different isomers of heterodimer **5** (**5a**−**5h**) have been located on the PES. However, the most stable isomer of **5** is **5d**, which is calculated to be −33.2 kcal mol^{-1} more stable than the separate reactants (Table 4). In this isomer the CO_2 moiety has inserted into the N(2)−Li(2) bond.

Table 4. Calculated relative Gibbs free energies [kcal mol^{-1}] of heterodimers **5a**−**h** (free and CO_2 and/or THF solvated) and transition structures **TS5**−**TS10** on the way to forming homodimers

Structure	BII//BI	BI//BI
4	0	0
5a	−	−21.6
5b	−21.9	−25.4
5c	−28.6	−31.4
5d	−33.2	−34.4
5e	−	−29.0
5f	−26.8	−28.3
5g	−	−30.0
5h	−	−21.7
5b−**(THF)**	−	−29.6
5d−**(THF)**	−32.9	−38.5
5d−**(THF)$_2$**	−29.6	−40.2
5g−**(THF)**	−	−35.8
5g−**(THF)$_2$**	−	−34.2
5b−**(CO$_2$)**	−	−23.7
5c−**(CO$_2$)**	−23.2	−28.7
5d−**(CO$_2$)**	−29.1	−34.0
5f−**(CO$_2$)**	−	−28.8
5g−**(CO$_2$)**	−	−30.3
5d−**(CO$_2$)**−**(THF)**	−27.1	−36.8
TS5	−23.5	−27.6
TS6	−16.4	−21.2
TS7	−18.2	−24.3
TS8	−13.3	−19.9
TS9	−20.5	−29.7
TS10	−20.5	−29.6

In **5d**, an almost planar six-membered ring is formed in which the two carbamate oxygen atoms coordinate one lithium atom each, and the amide nitrogen atom coordinates both lithium atoms (Figure 6). The amine nitrogen atom from the lithium amide monomer additionally coordinates one of the lithium cations, while the amine nitrogen atom from the lithium carbamate is not part of the lithium coordination sphere. The structural differences between the isomers of the **5** series are mostly found in the amine nitrogen and carbamate oxygen coordination to the two lithium cations. At this point we anticipate that coordination between the lithium and amine-nitrogen atoms, both in the lithium amide and in the lithium carbamate, can also be of importance for dynamic processes in which the exchange of solvent molecules coordinating the lithium cations is involved. The computational studies of the isomerisation processes between structures **5a**−**5h** (which are presumably separated by small activation barriers) are therefore immensely difficult, and thus have not been the objectives of this study.

Solvation of isomer **5d** by one THF molecule results in a net destabilisation of +0.3 kcal mol^{-1}, calculated at the BII//BI level of theory (Figure 7). Further solvation leads to increased destabilisation (+3.3 kcal mol^{-1}). Using the BI//BI approach, **5d**−**(THF)$_2$** is the most stable compound, which indicates that in a THF solution the isomers **5d**, **5d**−**(THF)** and **5d**−**(THF)$_2$** are in equilibrium. Other solvated isomers of **5** are found to be less stable than **5d**−**(THF)**, see Table 4.

Formation of Homodimers of the Lithium Carbamate

Addition of a second CO_2 molecule to the heterodimer **5** leads to the formation of the homodimer **6** of the lithium carbamate **1** (Scheme 3).

Initially, CO_2 acts as a solvent for lithium forming an encounter complex **5**−**(CO$_2$)**, of which several different isomers were located on the PES (Figure 8).

The most stable isomer is found to be **5d**−**(CO$_2$)** (see Table 4). However, the free energy for CO_2 solvation is cal-

 © 2004 Wiley-VCH Verlag GmbH & Co. KGaA, Weinheim

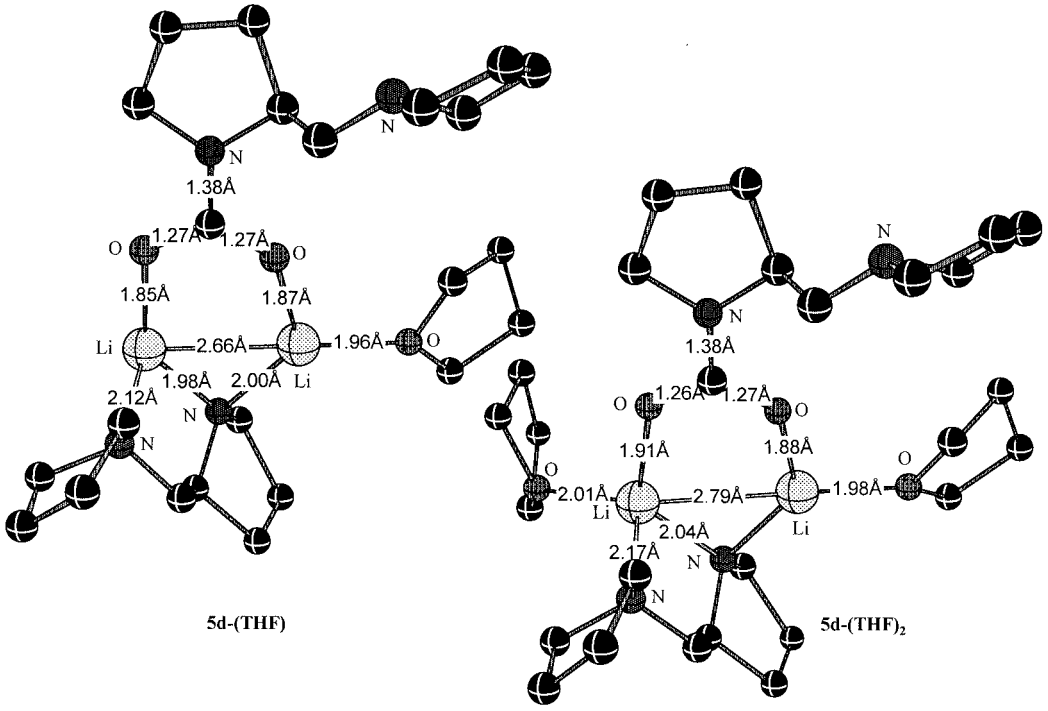

Figure 7. Optimised THF solvated heterodimers **5d**, cf. Figure 6

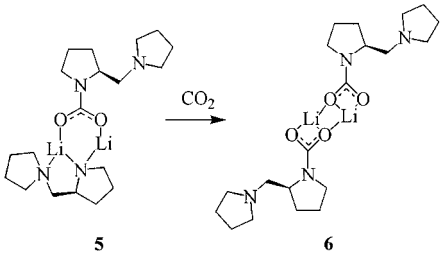

Scheme 3. Formation of homodimer **6** from heterodimer **5** and carbon dioxide

culated to be +4.1 kcal mol^{-1}, a similar magnitude to that for **3**. In some isomers of **5−(CO$_2$)** the distance between the CO_2 carbon atom and one of the carbamate oxygen atoms is rather short (about 2.5−2.8 Å; Figure 8). This indicated the possibility of another reaction path from the heterodimer, i.e. insertion into the O−Li bond rather than the N−Li bond. However, no such reaction paths or stable products thereof could be located using DFT methods, and therefore such a reaction does not appear to be very realistic for that type of a heterodimer. Nevertheless, as indicated by our homodimer and monomer calculations

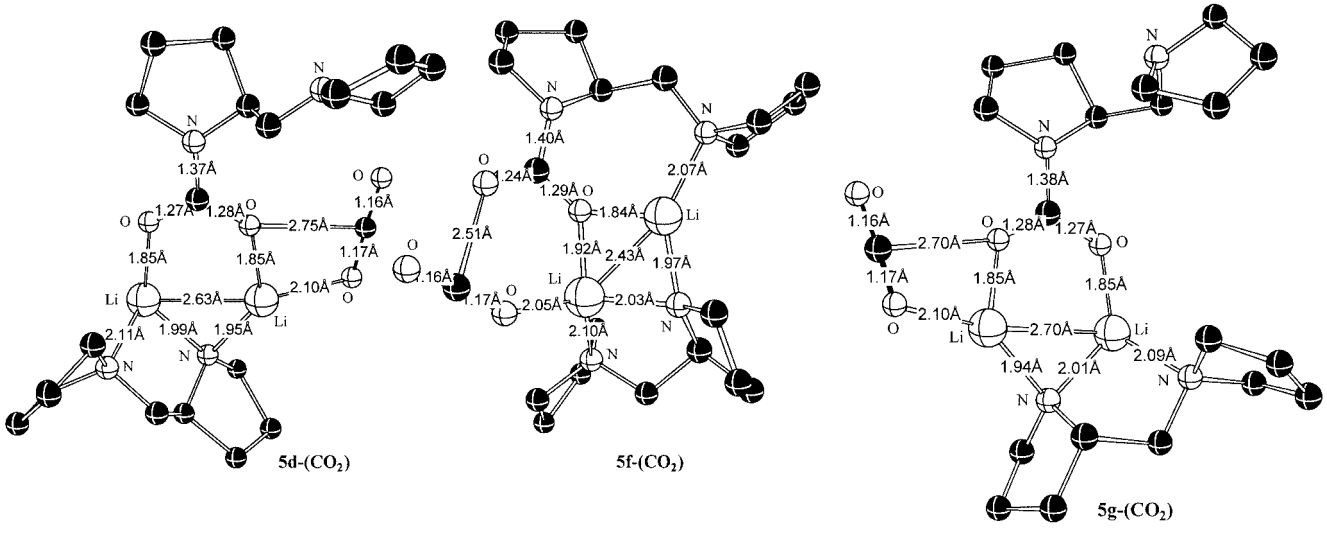

Figure 8. Optimised CO_2/heterodimer encounter complexes

 © 2004 Wiley-VCH Verlag GmbH & Co. KGaA, Weinheim

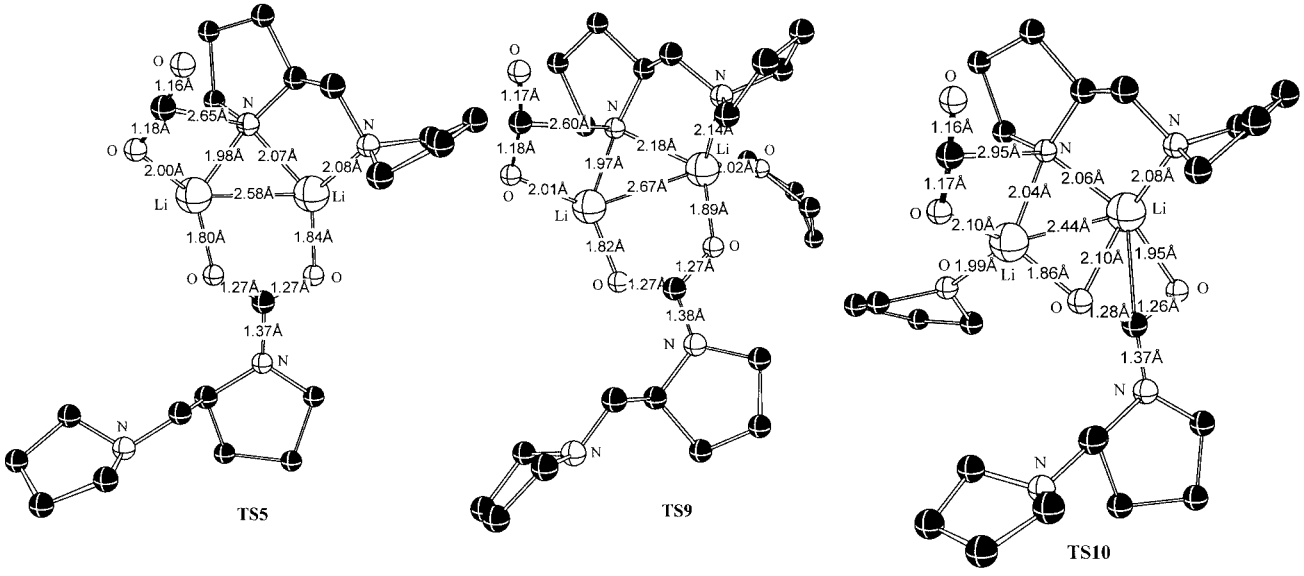

Figure 9. Optimised transition structures for the lithium carbamate homodimer formation from different encounter complexes **5−(CO$_2$)** and CO_2, cf. Figure 8

(cf. the paragraph "Further reaction paths" in Supporting Information), such a path cannot be excluded completely.

The different encounter complexes located were used to find TSs for formation of the homodimer **6** of the lithium carbamate **1**. Four different TSs for nucleophilic attack at CO_2 by an amide nitrogen were located, **TS5**−**TS8**, of which **TS5** is calculated to be the most stable (Figure 9 and Supporting Information).

The carbamate formation via **TS5** requires 5.6 kcal mol^{-1} from the initial complex **5d−(CO$_2$)** at the BII//BI level of theory. The calculated free energy activation barrier for **TS5** from reactant **4** and two molecules of CO_2 is −23.5 kcal mol^{-1}, while from **5d** it is 9.7 kcal mol^{-1} (Table 4 and Scheme 4). The other located TSs are at least 5.3 kcal mol^{-1} less stable than **TS5**.

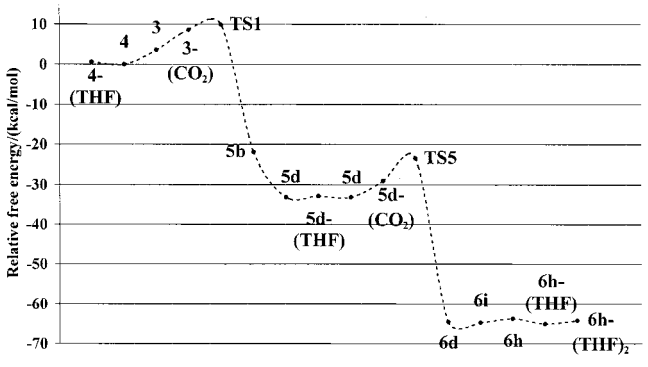

Scheme 4. Suggested preferred reaction pathway for lithium carbamate formation; free energies are calculated at the BII//BI level of theory and are relative to the dimer **4**, cf. Figure 1

THF solvation of the most stable TS **TS5** indicates that for this second step of CO_2 insertion, an equilibrium between solvated and unsolvated TSs is present. Both lithium cations in **TS5** were investigated by separate monosolvation giving the isomers **TS9** and **TS10** with nearly equal free energies of solvation (see Figure 9). In **TS10**, the unsolvated lithium features coordination to both oxygen atoms in the carbamate moiety, which differs from that observed in **TS5**. The four different unsolvated TSs (**TS5**−**TS8**) were found to lead to the formation of four different isomers in the homodimer family **6**. In addition, four other isomers were located on the PES (Figure 10 and Table 5). This, in combination with the small energy differences of all these isomers, again indicates the complexity of the systems involved in this study. In the dimers **6**, the second CO_2 moiety is inserted into a N−Li bond.

Among the different isomers of the homodimer **6**, isomers **6d**, **6h** and **6i** were found to be the most stable, and these structures are depicted in Figure 10, while the others can be found in the Supporting Information. The most stable isomers differ in the sense that **6h** and **6i** are ladder-like dimers in which *each* lithium cation is coordinated to one carbamate monomer in a bidentate fashion and to the other monomer through one of the oxygen anions; thus they are only coordinated to oxygen atoms. The "ladder-system" is found to be remarkably flat. The major difference between **6h** and **6i** is the manner in which the two monomers are coordinated; **6h** can be viewed as left-coordinated and **6i** as right-coordinated. In **6d** on the other hand, *one* lithium ion is coordinated to oxygen atoms only as described above, while the *other* lithium cation is coordinated to one carbamate monomer in a monodentate fashion and also to an amine-nitrogen atom.

 © 2004 Wiley-VCH Verlag GmbH & Co. KGaA, Weinheim

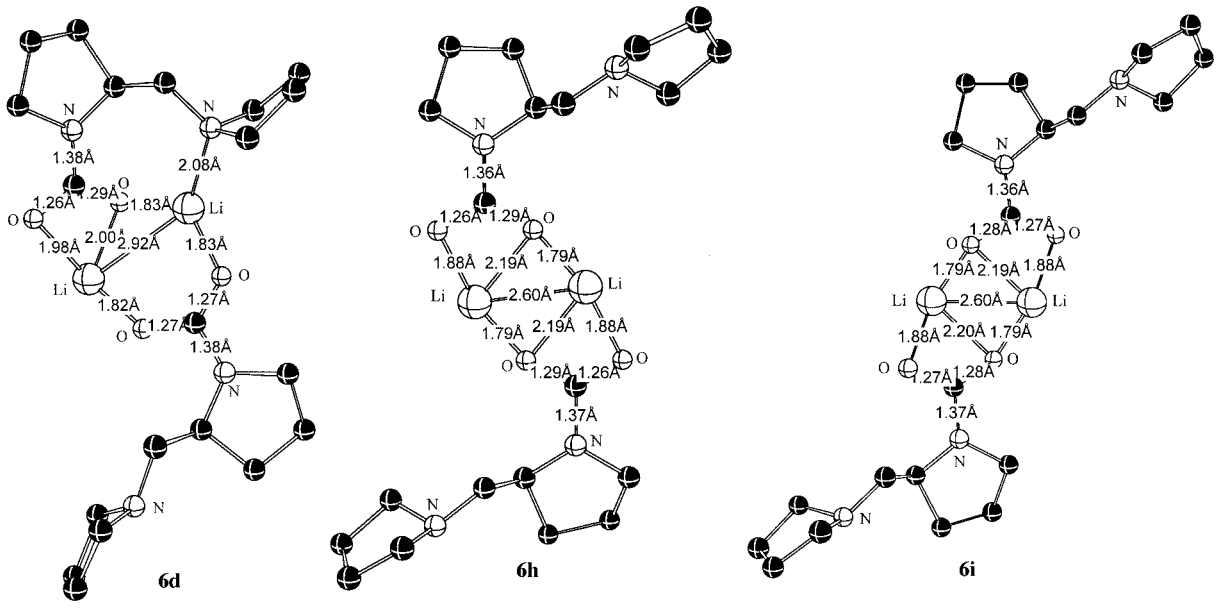

Figure 10. Optimised lithium carbamate homodimers **6**

Table 5. Calculated relative Gibbs free energies [kcal mol^{-1}] of the homodimers **6** (free and THF solvated)

Structure	BII//BI	BI//BI
4	0	0
6a	–	−62.3
6b	−43.8	−48.9
6c	–	−63.4
6d	−64.5	−67.8
6f	−59.1	−64.3
6g	−58.2	−62.8
6h	−63.7	−66.2
6i	−64.7	−67.0
6a−(THF)	–	−65.1
6d−(THF)	−62.5	−71.5
6g−(THF)	–	−59.0
6h−(THF)	−65.0	−71.3
6h−(THF)$_2$	−64.2	−75.4

THF solvation of **6** causes a small stabilisation, or in some cases a destabilisation. Thus, **6d**, **6h**, **6i**, **6h−(THF)** and **6h−(THF)$_2$** are the most stable dimers of lithium carbamate **1** with a free energy difference of only 1.3 kcal mol^{-1} (Figure 11 and Table 5). In the disolvated isomer, the ladder-like construction of **6h** is broken and an eight-membered, boat-shaped ring consisting of four oxygen, two lithium and two carbon atoms is formed. Such boat-shaped, eight-membered ring structural motifs in lithium carbamates[57] and in lithium carboxylates[58] have previously been characterised by X-ray structural studies. In the monosolvated isomer **6h−(THF)**, only one of the rings in the ladder is broken, which indicates that this is a structural intermediate between **6h** and **6h−(THF)$_2$**.

Monomer−Dimer Equilibrium of Lithium Carbamate 1

In order to elucidate the thermodynamic preference between monomers and dimers of **1** (Scheme 5), several different isomers of the monomer have been included in this study (**1a**−**1d**; Figure 12 and Table 6). Some of the less stable monomer isomers can be found in the Supporting Information.

The most stable isomer is found to be **1d**, in which the lithium is dicoordinated by the two carbamate oxygen atoms.

Upon THF solvation, the disolvated lithium carbamate monomer **1d−(THF)$_2$** is preferred (Figure 13). It should be noted that the relative energies for the monomers given in Table 6 are quoted relative to the energy of dimer **4**; thus the true energy difference between monomeric isomers is calculated by multiplying this number with the factor one half. Further solvation as in **1d−(THF)$_3$** destabilises the isomer.

Interestingly, the calculated free energy for the dimerisation of **1** is found to be relatively high (−23.5 kcal mol^{-1}). Here, the most stable, solvated dimer **6h−(THF)** is compared with the most stable, solvated monomer **1d−(THF)$_2$**. These calculations clearly indicate that the dimer **6** is favoured over the monomer **1**. Furthermore, the aggregation of two monomers of the lithium amide with two monomers of the lithium carbamate which leads to the formation of two heterodimers, is preferred over the formation of the homodimers [see Equation (1)]. This means that there is no thermodynamic driving force to separate the heterodimer into monomers for further strongly exogenic reactions leading to homodimers.

$$\underset{0}{2\,\mathbf{5d} + 4\ \mathrm{THF}} \rightleftharpoons 2\,\mathbf{1d\text{-}(THF)} + 2\,\mathbf{2\text{-}(THF)} \rightleftharpoons \underset{+2.2}{\mathbf{4} + \mathbf{6h\text{-}(THF)} + 3\ \mathrm{THF}} \quad (1)$$

These results shed some new light on our preliminary study (^{6}Li-^{1}H HOESY experiments and cryoscopy measure-

 © 2004 Wiley-VCH Verlag GmbH & Co. KGaA, Weinheim

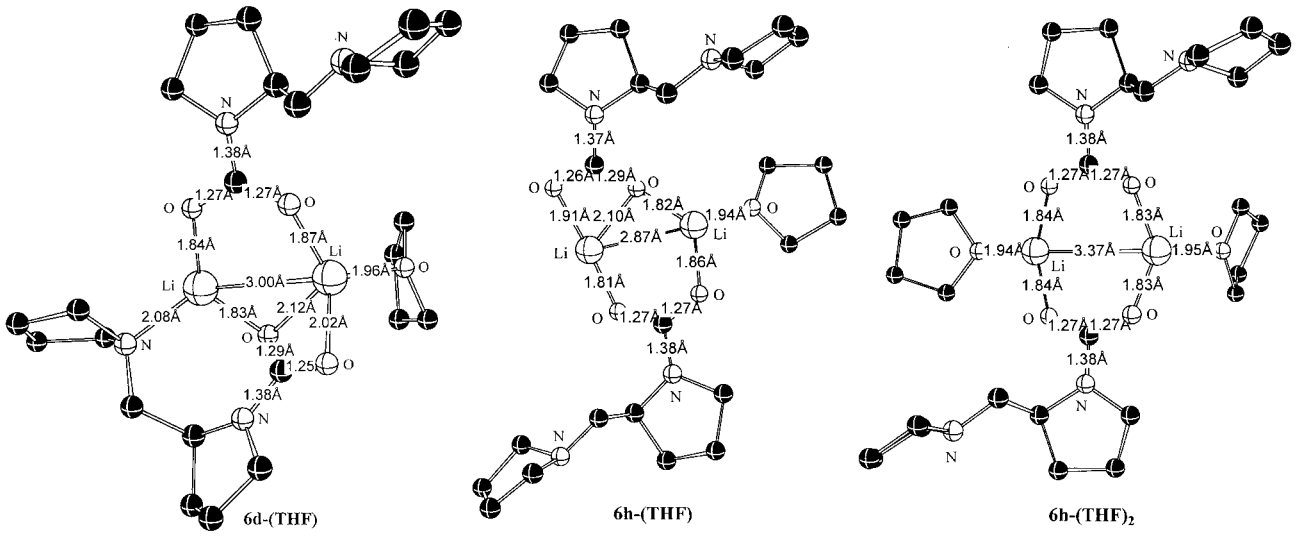

Figure 11. Optimised THF solvated lithium carbamate homodimers **6−(THF)$_x$** from their precursors **6**, cf. Figure 10

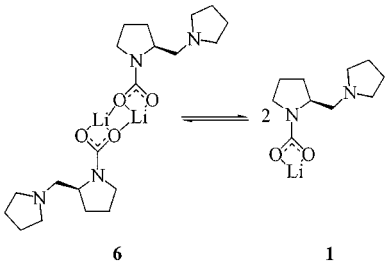

Scheme 5. Equilibrium between homodimer **6** and monomer of **1**

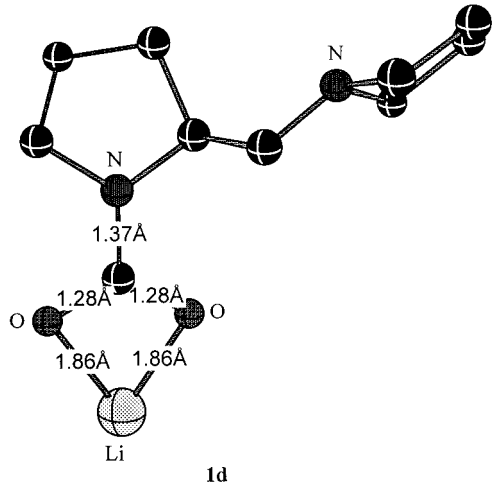

Figure 12. Optimised lithium carbamate monomer **1d**

ments[12]), which seemed to indicate that monomeric species exist to a significant extent in the equilibrium. In this previous study we reported on the monomeric structures **1b−(THF)$_2$** and **1d−(THF)$_2$**, and found that **1b−(THF)$_2$** is thermodynamically less stable than **1d−(THF)$_2$** but its structure is more consistent with the interpretations from the HOESY experiments. A plausible explanation that is in agreement with both the experiments and calculations is

Table 6. Calculated relative Gibbs free energies [kcal mol^{-1}] of the dimer (**6**) ⇄ monomer (**1**) equilibrium

Structure	BII//BI	BI//BI
4	0	0
6h−(THF)	−65.0	−71.3
1a	–	−11.1
1b	–	−8.2
1c	–	+14.6
1d	−27.1	−22.5
1a−(THF)	–	−35.0
1a−(THF)$_2$	−26.1	−43.1
1b−(THF)$_2$	−18.0	−34.1
1d−(THF)	–	−46.1
1d−(THF)$_2$	−41.5	−55.7
1d−(THF)$_3$	–	−48.4

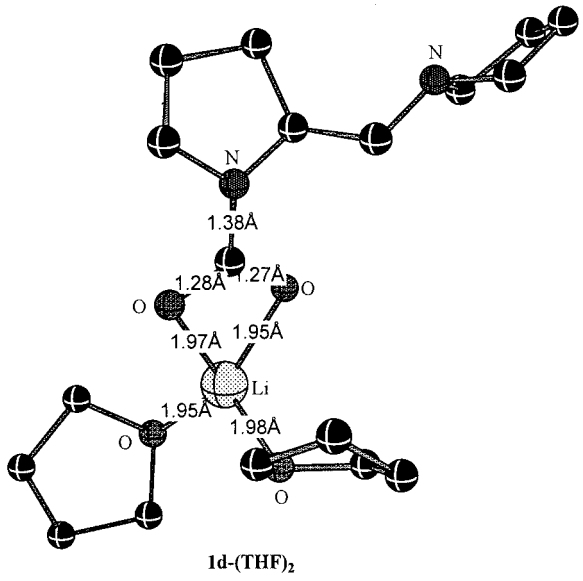

Figure 13. Optimised THF solvated lithium carbamate monomer **1d−(THF)$_2$**

 © 2004 Wiley-VCH Verlag GmbH & Co. KGaA, Weinheim

now presented. We suggest that the HOESY measurements have been performed on a *kinetically* preferred isomer containing the *structural motif* of **1b−(THF)$_2$**, e.g. isomer **6d** (c.f. Figure 14), rather than the thermodynamically most stable isomer **6h−(THF)**.

The product formation via **TS5**, the most stable TS for homodimer formation, leads to isomer **6d**. It should be noted that isomer **6d** is calculated to be only 0.5 kcal mol^{-1} less stable than **6h−(THF)**. Considering the accuracy of the DFT methods, the isomers should be seen as almost isoenergetic. In the optimised structure of isomer **6d**, as shown in Figure 14, the upper part contains the structural motif of **1b**. Short Li−H distances (< 3.5 Å) to the hydrogen atoms at C2 and C2′/C5′ are detected, which are in agreement with the HOESY measurements reported in our previous paper. On the other hand, the short distances to the hydrogen atoms at C5 and C3′/C4′ as previously reported could not be found in the conformations calculated here (for atom numbering, see Scheme 1). As such interactions are characteristic for structures which − e.g. starting with **6d** − with great certainty can be interconverted by energetically inexpensive conformational changes, they belong to a very flat part of the conformational energy surface. As expected, in the related thermodynamically preferred "ladder-like" isomers **6h** and **6i** no short Li−H distances could be detected. Thus, they are not the dominant isomers on which the HOESY-measurements have been performed.

Conclusion

In this study, we have computationally investigated reaction mechanisms for the formation of chiral lithium carbamates from chiral lithium amides and CO_2. The lithium amide **2** exists as a mixture of THF solvated and unsolvated dimers. There is a slight preference for dimer **4**, which possesses equivalent lithium cations. We conclude from our investigations that the fixation of carbon dioxide through the formation of the lithium carbamate follows a two-step mechanism. Each step inserts one CO_2 molecule into a nitrogen−lithium bond of a lithium amide dimer (Scheme 4). Initial addition of carbon dioxide to the reagent leads to two almost isoenergetic encounter complexes **3−(CO$_2$)** and **4−(CO$_2$)**; the former is preferred by only ca. 1 kcal mol^{-1}. From **3−(CO$_2$)**, this exergonic reaction proceeds over a small activation barrier (ca. 10 kcal mol^{-1}) to give the heterodimers **5** that are composed of one lithium amide and one lithium carbamate. Interestingly, it is found that the TSs without solvent coordination to the lithium cation are more stable than those in which solvent molecules have been incorporated. Addition of a second carbon dioxide molecule to the heterodimer then leads to the encounter complex **5d−(CO$_2$)**. Several homodimers **6** of the lithium carbamate **1** are formed from **5d−(CO$_2$)** after overcoming a small activation barrier (ca. 5 kcal mol^{-1}).

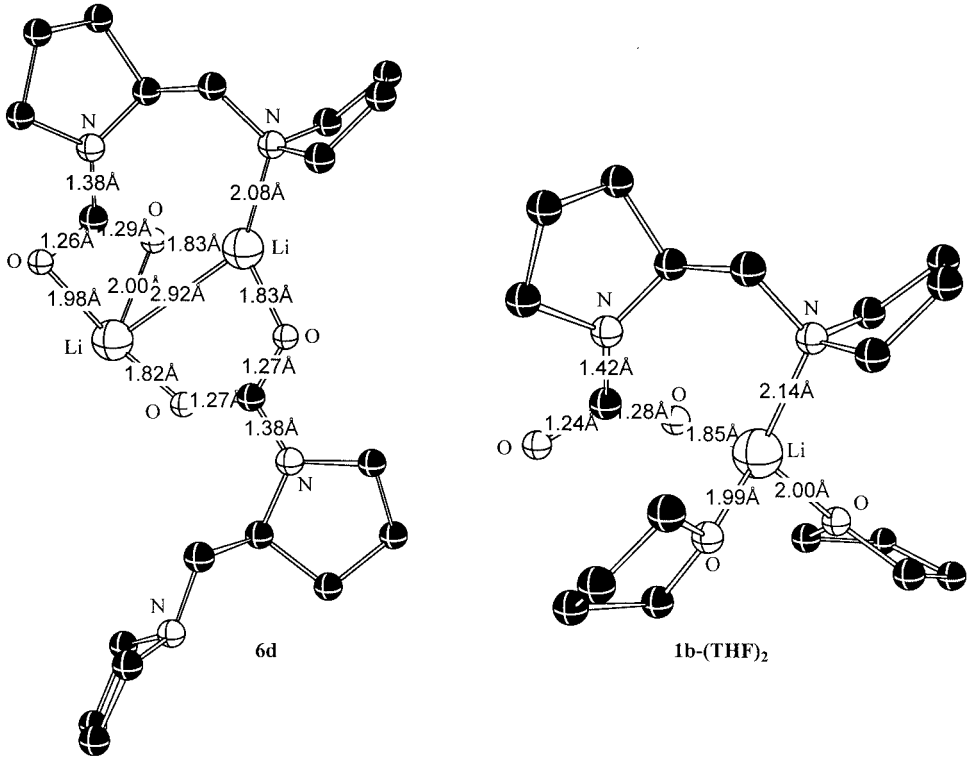

Figure 14. Structural motif similarities between lithium carbamate **6d** dimer and the monomer **1b−(THF)$_2$**

 © 2004 Wiley-VCH Verlag GmbH & Co. KGaA, Weinheim

The rate determining step is computationally determined to be the *first* CO_2 insertion reaction. A multitude of isomers of both the hetero- and the homodimers were localised and we propose that several isomers of **6** and of **1** will coexist in solution. However, when thermodynamic equilibrium conditions are present, the concentration of the monomers of **1** can be expected to be quite low. Finally, in the course of our systematic investigations we detected a novel CO_2 fixation mode − the insertion of this cumulene into O−Li bonds of carbamates, cf. Supporting Information. In contrast with the formation of the most stable homodimer isomers **6d** and **6h−(THF)**, the formation of insertion products such as **7** is endergonic (+21 kcal mol^{-1} relative to **6** + CO_2). At present, such reaction paths appear to be of minor importance.

We think that the investigation presented here could serve − due to its predictive power based on high-level DFT calculations − as a useful tool for designing other metal-mediated reactions that can be employed for the fixation of cumulenes and/or heterocumulenes.

Acknowledgments

S. O. N. L. gratefully acknowledges a post-doctoral stipend from the Wenner-Gren Foundation, Sweden. Financial support by the Deutsche Forschungsgemeinschaft (Sonderforschungsbereich 436) and by the Thüringer Ministerium für Wissenschaft, Forschung und Kultur (Erfurt, Germany) is gratefully acknowledged.

[1] X. C. Sun, Y. Z. Zhang, D. Zeckner, W. Current, S. H. Chen, *Bioorg. Med. Chem. Lett.* **2001**, *11*, 3055−3059.
[2] X. C. Sun, M. Rodriguez, D. Zeckner, B. Sachs, W. Current, R. Boyer, J. Paschal, C. McMillian, S. H. Chen, *J. Med. Chem.* **2001**, *44*, 2671−2674.
[3] F. M. H. de Groot, L. W. A. van Berkom, H. W. Scheeren, *J. Med. Chem.* **2000**, *43*, 3093−3102.
[4] S. M. Rahmathullah, J. E. Hall, B. C. Bender, D. R. McCurdy, R. R. Tidwell, D. W. Boykin, *J. Med. Chem.* **1999**, *42*, 3994−4000.
[5] E. W. Ng, M. M. Aung, M. E. Abood, B. R. Martin, R. K. Razdan, *J. Med. Chem.* **1999**, *42*, 1975−1981.
[6] P. V. Attwood, J. C. Wallace, *Acc. Chem. Res.* **2002**, *35*, 113−120.
[7] M. Feroci, A. Inesi, L. Rossi, *Tetrahedron Lett.* **2000**, *41*, 963−966.
[8] M. Feroci, M. A. Casadei, M. Orsini, L. Palombi, A. Inesi, *J. Org. Chem.* **2003**, *68*, 1548−1551.
[9] R. N. Salvatore, V. L. Flanders, D. Ha, K. W. Jung, *Org. Lett.* **2000**, *2*, 2797−2800.
[10] R. N. Salvatore, S. I. Shin, A. S. Nagle, K. W. Jung, *J. Org. Chem.* **2001**, *66*, 1035−1037.
[11] M. Amedjkouh, P. Ahlberg, *Tetrahedron: Asymmetry* **2002**, *13*, 2229−2234.
[12] U. Köhn, E. Anders, *Tetrahedron Lett.* **2002**, *43*, 9585−9589.
[13] Y. Otsuji, M. Arakawa, N. Matsumura, E. Haruki, *Chem. Lett.* **1973**, 1193−1196.
[14] E. Haruki, M. Arakawa, N. Matsumura, Y. Otsuji, E. Imoto, *Chem. Lett.* **1974**, 427−428.
[15] N. Matsumura, T. Ohba, S. Yoneda, *Chem. Lett.* **1983**, 317−318.
[16] S. O. Nilsson Lill, E. Anders, U. Köhn, *2nd International SFB Congress, Metal Mediated Reactions Modelled After Nature* (Jena, Germany) **2002**.
[17] S. Benetti, R. Romagnoli, C. De Risi, G. Spalluto, V. Zanirato, *Chem. Rev. (Washington, DC, U. S.)* **1995**, *95*, 1065−1114.
[18] T. Mukaiyama, K. Soai, T. Sato, H. Shimizu, K. Suzuki, *J. Am. Chem. Soc.* **1979**, *101*, 1455−1460.
[19] L. Colombo, C. Gennari, G. Poli, C. Scolastico, *Tetrahedron* **1982**, *38*, 2725−2727.
[20] T. Mukaiyama, M. Asami, *Top. Curr. Chem.* **1985**, *127*, 133−167.
[21] M. Asami, *Bull. Chem. Soc. Jpn.* **1990**, *63*, 721−727.
[22] S. Kobayashi, H. Uchiro, Y. Fujishita, I. Shiina, T. Mukaiyama, *J. Am. Chem. Soc.* **1991**, *113*, 4247−4252.
[23] D. Enders, S. F. Muller, G. Raabe, J. Runsink, *Eur. J. Org. Chem.* **2000**, 879−892.
[24] D. Enders, H. Kipphardt, P. Gerdes, L. J. Brenavalle, V. Bhushan, *Bull. Soc. Chim. Belg.* **1988**, *97*, 691−704.
[25] M. J. Frisch, G. W. Trucks, H. B. Schlegel, G. E. Scuseria, M. A. Robb, J. R. Cheeseman, V. G. Zakrzewski, J. A. Montgomery Jr., R. E. Stratmann, J. C. Burant, S. Dapprich, J. M. Millam, A. D. Daniels, K. N. Kudin, M. C. Strain, O. Farkas, J. Tomasi, V. Barone, M. Cossi, R. Cammi, B. Mennucci, C. Pomelli, C. Adamo, S. Clifford, J. Ochterski, G. A. Petersson, P. Y. Ayala, Q. Cui, K. Morokuma, D. K. Malick, A. D. Rabuck, K. Raghavachari, J. B. Foresman, J. Cioslowski, J. V. Ortiz, B. B. Stefanov, G. Liu, A. Liashenko, P. Piskorz, I. Komaromi, R. Gomperts, R. L. Martin, D. J. Fox, T. Keith, M. A. Al-Laham, C. Y. Peng, A. Nanayakkara, C. Gonzalez, M. Challacombe, P. M. W. Gill, B. Johnson, W. Chen, M. W. Wong, J. L. Andres, C. Gonzalez, M. Head-Gordon, E. S. Replogle, J. A. Pople, *GAUSSIAN 98, Rev. A7*, Pittsburgh, PA, Gaussian Inc., **1998**.
[26] G. Schaftenaar, J. H. Noordik, *J. Comput.-Aided Mol. Des.* **2000**, *14*, 123−134.
[27] A. D. Becke, *J. Chem. Phys.* **1993**, *98*, 5648−5652.
[28] C. Lee, W. Yang, R. G. Parr, *Phys. Rev. B: Condens. Matter* **1988**, *37*, 785−789.
[29] A. Schaefer, H. Horn, R. Ahlrichs, *J. Chem. Phys.* **1992**, *97*, 2571−2577.
[30] P. C. Hariharan, J. A. Pople, *Theor. Chim. Acta* **1973**, *28*, 213−222.
[31] T. Clark, J. Chandrasekhar, G. W. Spitznagel, P. v. R. Schleyer, *J. Comput. Chem.* **1983**, *4*, 294−301.
[32] G. W. Spitznagel, T. Clark, J. Chandrasekhar, P. v. R. Schleyer, *J. Comput. Chem.* **1982**, *3*, 363−371.
[33] J. Chandrasekhar, J. G. Andrade, P. v. R. Schleyer, *J. Am. Chem. Soc.* **1981**, *103*, 5609−5612.
[34] Thermochemistry calculations were performed using the standard routine in Gaussian 98, Version A7 (for details cf. Gaussian 98 User's Reference, Gaussian Inc., Carnegie Office Park, Building 6, Pittsburgh, PA, USA) or the *freqchk* routine in conjunction with the final checkpoint file resulting from successful frequency calculations. For a brief introduction see: J. W. Ochterski, *Thermochemistry in Gaussian*, **2000**, http://www.gaussian.com/g_whitepap/thermo/thermo.pdf, or J. W. Ochterski, *Vibrational Analysis in Gaussian*, **1999**, http://www.gaussian.com/g_whitepap/vib/vib.pdf.
[35] C. Møller, M. S. Plesset, *Phys. Rev.* **1934**, *46*, 618−622.
[36] B. J. Lynch, P. L. Fast, M. Harris, D. G. Truhlar, *J. Phys. Chem. A* **2000**, *104*, 4811−4815.
[37] K. Gregory, P. v. R. Schleyer, R. Snaith in *Adv. Inorg. Chem.* (Ed. A. G. Sykes), Academic Press, London, **1991**, pp. 47−142.
[38] W. N. Setzer, P. v. R. Schleyer in *Adv. Organomet. Chem.* (Ed. A. G. Sykes), Academic Press, London, **1985**, pp. 353−451.
[39] R. E. Mulvey, *Chem. Soc. Rev.* **1991**, *20*, 167−209.
[40] R. E. Mulvey, *Chem. Soc. Rev.* **1998**, *27*, 339−346.
[41] F. Pauer, P. P. Power in *Lithium Chemistry: A theoretical and experimental overview* (Eds. A. M. Sapse, P. v. R. Schleyer), John Wiley & Sons, Inc., New York, **1995**, pp. 595.
[42] G. Hilmersson, P. I. Arvidsson, Ö. Davidsson, M. Håkansson, *Organometallics* **1997**, *16*, 3352−3362.
[43] G. Hilmersson, P. I. Arvidsson, Ö. Davidsson, M. Håkansson, *J. Am. Chem. Soc.* **1998**, *120*, 8143−8149.
[44] P. I. Arvidsson, G. Hilmersson, P. Ahlberg, *J. Am. Chem. Soc.* **1999**, *121*, 1883−1887.

 © 2004 Wiley-VCH Verlag GmbH & Co. KGaA, Weinheim

[45] P. I. Arvidsson, Ö. Davidsson, *Angew. Chem. Int. Ed.* **2000**, *39*, 1467−1469.
[46] A.-M. Sapse, P. v. R. Schleyer, *Lithium Chemistry: A Theoretical and Experimental Overview*, John Wiley & Sons, Inc., New York, **1995**, pp. 595.
[47] D. Pettersen, M. Amedjkouh, S. O. Nilsson Lill, K. Dahlén, P. Ahlberg, *J. Chem. Soc., Perkin Trans. 2* **2001**, 1654−1661.
[48] F. E. Romesberg, D. B. Collum, *J. Am. Chem. Soc.* **1992**, *114*, 2112−2121.
[49] N. D. R. Barnett, R. E. Mulvey, W. Clegg, P. A. O′Neil, *J. Am. Chem. Soc.* **1991**, *113*, 8187−8188.
[50] M. P. Bernstein, F. E. Romesberg, D. J. Fuller, A. T. Harrison, D. B. Collum, Q. Y. Liu, P. G. Williard, *J. Am. Chem. Soc.* **1992**, *114*, 5100−5110.
[51] A. Johansson, Ö. Davidsson, *Chem. Eur. J.* **2001**, *7*, 3461−3465.
[52] A. Johansson, Ö. Davidsson, *Organometallics* **2001**, *20*, 4185−4189.
[53] A. Johansson, A. Pettersson, Ö. Davidsson, *J. Organomet. Chem.* **2000**, *608*, 153−163.
[54] A. Abbotto, A. Streitwieser, P. v. R. Schleyer, *J. Am. Chem. Soc.* **1997**, *119*, 11255−11268.
[55] S. M. Bachrach, A. Streitwieser Jr., *J. Am. Chem. Soc.* **1984**, *106*, 2283−2287.
[56] B. J. Lynch, Y. Zhao, D. G. Truhlar, *J. Phys. Chem. A* **2003**, *107*, 1384−1388.
[57] R. P. Davies, P. R. Raithby, R. Snaith, *Organometallics* **1996**, *15*, 4355−4356.
[58] G. Smith, E. J. O′Reilly, C. H. L. Kennard, *Acta Crystallogr., Sect. C* **1986**, *42*, 1329−1331.
[59] Z. W. Liu, M. Torrent, K. Morokuma, *Organometallics* **2002**, *21*, 1056−1071.

Received March 11, 2004

 © 2004 Wiley-VCH Verlag GmbH & Co. KGaA, Weinheim